Pure Appl. Chem., Vol. 82, No. 4, pp. 891–904, 2010.
doi:10.1351/PAC-CON-09-09-04

Toward carbyne: Synthesis and stability of really long polyynes*

Rik R. Tykwinski[1,2,‡], Wesley Chalifoux[2], Sara Eisler[3], Andrea Lucotti[4], Matteo Tommasini[4], Daniele Fazzi[5], Mirella Del Zoppo[4], and Giuseppe Zerbi[4]

[1]Institute for Organic Chemistry, Friedrich-Alexander-University, Erlangen-Nürnberg, Henkestrasse 42, 91054 Erlangen, Germany; [2]Department of Chemistry, University of Alberta, Edmonton, Alberta T6G 2G2, Canada; [3]Department of Chemistry, University of New Brunswick, Fredericton, New Brunswick, E3B 5A3, Canada; [4]Department of Chemistry, Materials and Chemical Engineering "G. Natta", Politecnico di Milano, Piazza Leonardo da Vinci 32, 20133 Milan, Italy; [5]Center for NanoScience and Technology CNST IIT@PoliMi, via Pascoli 70/3, 20133 Milan, Italy

Abstract: Molecules composed of sp-hybridized carbon chains (polyynes) are the simplest of the known conjugated organic oligomers. In comparison to their counterparts such as polyacetylene and polydiacetylene, however, the formation of polyynes has traditionally posed a difficult synthetic challenge. In particular, there is no reliable method to form end-capped polyethynylene, and monodisperse polyynes have therefore been assembled. As a result, structure–property relationships for shorter polyynes have been relatively well established in recent years, while extension of these trends toward longer polyynes has remained a difficult task. Using the Fritsch–Buttenberg–Wiechell (FBW) rearrangement, the formation of diynes through decaynes has become possible and has provided a unique chance to explore the physical characteristics of conjugated polyyne chains. This paper highlights recent advances in the synthesis of extended polyynes, as well as interesting aspects of their NMR, Raman, and UV/vis spectroscopic analyses. These synthetic achievements offer the opportunity to predict some of the properties of the carbon allotrope carbyne. In particular, a set of X-ray crystallographic analyses of *t*-Bu end-capped polyynes (**tBu[*n*]**) shows a definitive experimental trend in reduced bond-length alternation (BLA).

Keywords: alkylidene carbenes; alkynes; carbyne; conjugated oligomers; Peierls distortion; polyynes; Raman spectroscopy.

INTRODUCTION

Many aspects of modern science depend on the chemistry and properties of the various forms of pure carbon, including diamond (sp^3-hybridized carbon) and graphite/graphene (sp^2-hybridized carbon), as well as the more recent studies of fullerenes and nanotubes [1]. Extending this trend to sp-hybridized carbon leads to the compound/material often referred to as carbyne [2]. The existence, structure, and properties of carbyne have been a topic of some discussion [3–5], but this account will not attempt to

Pure Appl. Chem.* **82, 757–1063 (2010). An issue of reviews and research papers based on lectures presented at the 13th International Symposium on Novel Aromatic Compounds (ISNA-13), 19–24 July 2009, Luxembourg City, Luxembourg on the theme of aromaticity.
‡Corresponding author

reconcile the various interpretations/opinions that have played a role in this debate. Rather, a straightforward approach toward approximating the properties of carbyne will be described, based on one of the most common approaches available to the synthetic chemist: the oligomer approach [6,7]. This scheme is not a new one. Some 50 years ago, Bohlmann had explored the synthesis of polyynes end-capped with *tert*-butyl groups, including **tBu[2]** through **tBu[7]** (Fig. 1) [8]. The **tBu[*n*]** series then received the attention of Jones and co-workers, who successfully produced **tBu[8]** and **tBu[10]** [9]. Finally, in 1972 the efforts of Walton and co-workers produced both **tBu[10]** and **tBu[12]** [10]. Around nearly the same time, this group also reported a series of polyynes based on end-capping with triethylsilyl groups, which culminated at the formation of **TES[16]** [11]. Even though **TES[16]** was contaminated with TES–$[C{\equiv}C]_8$–H as a result of incomplete homocoupling, it could be characterized by UV/vis spectroscopy and remains the longest polyyne reported to date. More recently, Cox and co-workers have reported the only known dodecayne that features aryl endgroups (**Ar[12]**), although the molecule proved to be quite unstable and could be characterized only by UV/vis spectroscopy and mass spectrometry (MS) [12]. Thus, there has been a growing body of work on polyyne molecules [13–15], but nevertheless little is known of polyynes with greater than 10 contiguous acetylene units. The landmark studies in this area have only recently appeared and originated from the fantastic work of Gladysz and co-workers using Pt-end-capped polyynes. Their synthetic efforts provide the first opportunity to study polyynes beyond the length of 20 carbons, through the formation of stable derivatives including **Pt[10]**, **Pt[12]**, and **Pt[14]** [16–18]. These derivatives have made possible the first real examination of

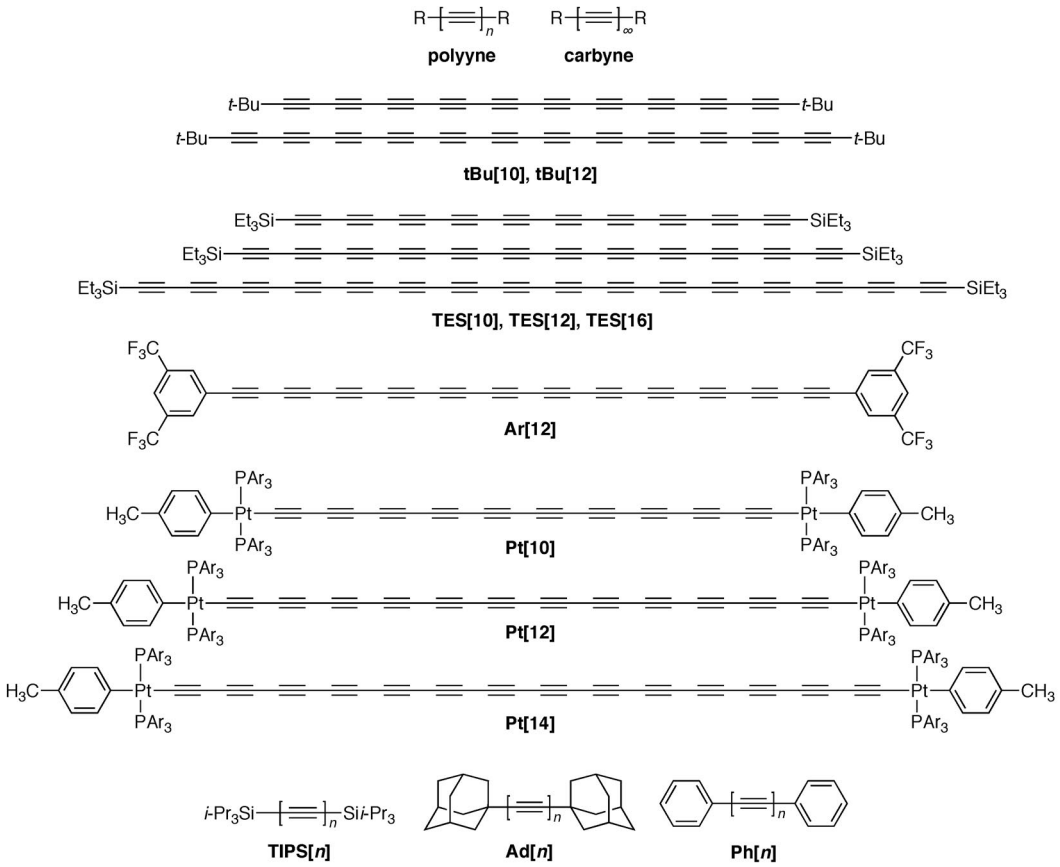

Fig. 1 Selected general chemical structures of polyynes discussed in this paper.

polyyne chains using a suite of modern spectroscopic techniques, and, in particular, the third-order nonlinear optical characteristics have been examined using the Z-scan technique over the wavelength range of 520–1500 nm [19].

The above description, albeit brief, provides a reasonably complete account of the major achievements in the formation and study of long polyynes and also sets the stage for the discussion of our work in this area [13]. From the onset, two primary objectives have dominated our approach to the study of carbyne. First and foremost, we have targeted polyynes with end-capping groups designed to interact as little as possible with the polyyne core, allowing for the best possible analysis of the polyyne carbon chain itself. Second, the development and optimization of the Fritsch–Buttenberg–Wiechell (FBW) rearrangement [20,21] has been a consistent focus in our work, in an attempt to minimize the necessity for generating long terminal acetylenes [22].

Initial synthetic efforts focused on the study of triisopropylsilyl [23,24] and adamantyl [25] end-capped series of polyynes (**TIPS[*n*]** and **Ad[*n*]**, respectively, Fig. 1), which provided an excellent description of the optical properties of polyynes up to **TIPS[10]** and **Ad[10]**. A brief foray was also made into the synthesis of **tBu[*n*]** polyynes [26] using the FBW rearrangement. This endeavor was also ultimately limited to the synthesis of the decayne (**tBu[10]**), but it nevertheless provided an unprecedented opportunity to study the correlation between bond-length alternation (BLA) and polyyne length. The present report will draw from these studies toward establishing the general structural and electronic characteristics of polyynes.

RESULTS AND DISCUSSION

Synthesis

In addition to the shorter derivatives **TIPS[2]–[4]**, the FBW approach to polyynes was also successful for the formation of longer polyynes **TIPS[6]**, **TIPS [8]**, and **TIPS[10]** [23,24,27]. The approach could best be described as semi-optimized: it provided reasonable quantities of each polyyne for study, but the overall protocol was disappointingly time-consuming. As a result, attempts were made to optimize the general approach using the **Ad[*n*]** series of molecules, and a simplified synthetic scheme was devised that derived from 3-adamantyl-2-propynoic acid [25]. Subsequently, an analogous approach was also used for the assembly of the *t*-Bu series through **tBu[10]** [26], as exemplified in Schemes 1 and 2. The syntheses of diyne **tBu[2]** [28] and tetrayne **tBu[4]** were easily accomplished via oxidative homocoupling of *t*-Bu-acetylene and *t*-Bu-butadiyne, respectively (not shown). Triyne **tBu[3]** was assembled in the manner reported for other symmetrical triynes [29,30], beginning with reaction of *t*-Bu-C≡CLi with ethyl formate to give the diyne alcohol. The alcohol was oxidized to the ketone, which was then converted to the dibromoolefin using the method of Ramirez [31]. An FBW rearrangement then gave the desired product.

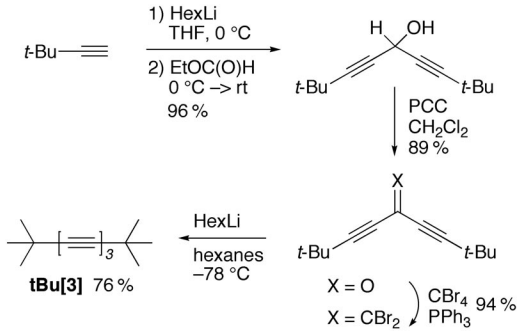

Scheme 1 Synthesis of the *t*-Bu end-capped triyne (**tBu[3]**).

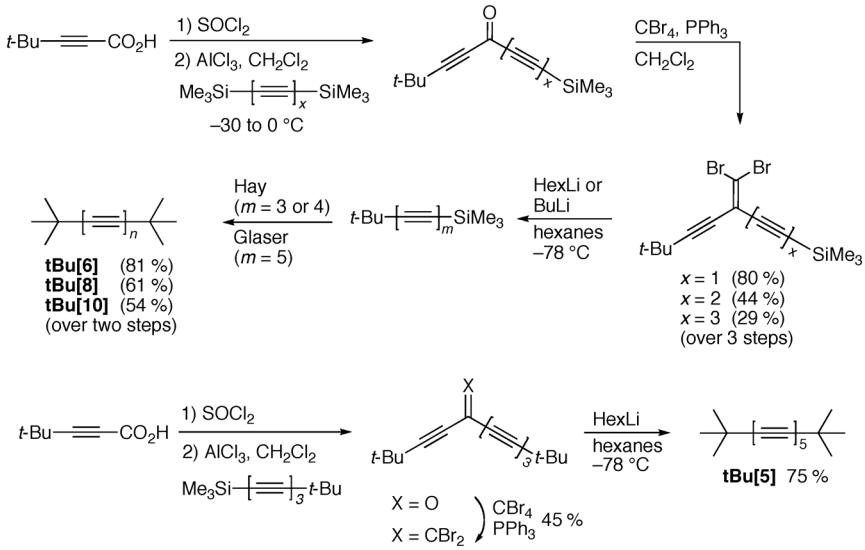

Scheme 2 Synthesis of *t*-Bu end-capped penta-, hexa-, octa-, and decaynes.

The synthesis of **tBu[6]**, **tBu[8]**, and **tBu[10]** has been used to illustrate the divergent nature of the improved protocol. All three derivatives derived from a sequence of synthetic steps (Scheme 2) starting from *t*-Bu-C≡CCO_2H [32]. Following conversion of the acid to the acid chloride with thionyl chloride, an acylation reaction with the appropriate α,ω-bis(trimethylsilyl)polyyne [33] gave the corresponding ketone. Given their limited stability, the ketones were carried on directly to the dibromoolefination step following purification by passing through a short column of silica gel. With the dibromoolefins in hand, an FBW rearrangement then gave the expected tri-, tetra-, or pentayne intermediates. Following aqueous work-up, the tri- and tetrayne precursors were subjected directly to Hay oxidative homocoupling (THF, MeOH, CuCl, TMEDA, O_2) [34]. Under these conditions, the TMS-protecting group was successfully removed and homocoupling afforded **tBu[6]** or **tBu[8]** in acceptable yield. Attempts to use this same procedure with the analogous pentayne led not only to the desired product **tBu[10]**, but also nonayne **tBu[9]**. The apparent loss of acetylene during the course of a Hay coupling has been previously observed in both our work as well as that of Hirsch [24,35]. Unfortunately, the mechanism of this potentially interesting process remains unknown. In any case, changing the catalyst system to that of Eglinton–Glaser [$Cu(OAc)_2 \cdot H_2O$, THF, MeOH, pyridine] [36], prevented nonayne formation and gave the decayne **tBu[10]** in 54 % yield. As observed with the formation of **Ad[*n*]** and **TIPS[*n*]** series, product stability becomes an issue as one progresses to the length of the decayne. For example, **tBu[10]** can be isolated as a solid via solvent removal in vacuo, and the resulting product can be handled for a short period of time under ambient conditions (i.e., minutes) before significant decomposition occurs. However, as time persists the polyyne gradually darkens and turns black. **Caution**: Heat should be avoided, as **tBu[10]** exploded when contacted with a hot glass sampler used for electron impact-mass spectrometry (EI-MS) analysis (as an important note, it is best to treat all polyynes as though they might be explosive, especially under any type of heating or pressure). Crystallization of decayne **tBu[10]** could be achieved via slow evaporation of a CH_2Cl_2 solution kept at ca. 4 °C, which provided a crystalline solid that remained unchanged for weeks while under refrigeration at ca. 4 °C and was equally stable for months stored at ca. –20 °C. Finally, pentayne **tBu[5]** was formed in a similar fashion, simply by substituting Me_3Si-[C≡C]$_3$-*t*-Bu for Me_3Si-[C≡C]$_3$-$SiMe_3$ in the initial acylation reaction.

PHYSICAL AND SPECTROSCOPIC CHARACTERIZATION

The individual members of all three series (**TIPS[*n*]**, **Ad[*n*]**, **tBu[*n*]**) have been characterized by a variety of methods, often with an eye toward identifying saturation of a particular effect. For a particular set of oligomers, convergence of spectroscopic data vs. length to constant value (saturation) can shed light on the expected properties of the polymer carbyne. Alternatively, when saturation is not yet reached, extrapolation to the asymptotic limit of the data vs. length can also be used as a predictive tool. These modes of evaluating carbyne also depend, quite clearly, on the absence or reduction of end-group effects. While the electronic impact of the terminal groups has been minimized by the use of *i*-Pr_3Si, *t*-Bu, and 1-adamantyl groups, it should be noted that effects of the end-capping group cannot be entirely eliminated.

NMR spectroscopy

^{13}C NMR spectroscopy of series **tBu[*n*]** shows a consistent trend in the observed chemical shifts as a function of length (Table 1), as has been described for several other homologous series of polyynes [18,24,35]. Specifically, the most deshielded resonance of the polyyne framework moves steadily downfield from 86.3 ppm (**tBu[2]**) to 89.6 ppm (**tBu[10]**). The most upfield signal of each polyyne, however, is found in a narrow range of 61.7–61.4 ppm, except for **tBu[2]** where it is found at 63.7 ppm. The remaining resonances converge toward a value of ca. 63 ppm as the length is increased, suggesting this would be a good approximation of the chemical shift of the acetylenic carbons of carbyne; both **Ad[*n*]** and **TIPS[*n*]** show analogous trends. Even at the stage of the decaynes **tBu[10]**, **Ad[10]**, and **TIPS[10]**, however, it is worth noting that a unique resonance is observed for each sp-hybridized carbon. Thus, these remain molecular species, i.e., saturation has not yet been achieved.

Table 1 Solution-state ^{13}C NMR spectroscopic data for the series **tBu[*n*]**.

Polyyne	^{13}C NMR chemical shifts $CDCl_3$ (ppm)
tBu[2]	86.3, 63.7, 30.6, 28.0
tBu[3]	87.0, 64.4, 61.4, 30.4, 28.1
tBu[4][a]	87.7 (C3), 64.5 (C4), 61.8 (C5), 61.5 (C6), 30.3, 28.2
tBu[5][a]	88.4 (C3), 64.4 (C4), 62.1 (C5), 62.0 (C6), 61.7 (C7), 30.2, 28.3
tBu[6]	88.8, 64.4, 62.5, 62.5, 61.9, 61.6, 30.2, 28.3
tBu[8]	89.4, 64.4, 63.4, 63.2, 62.9, 62.3, 61.7, 61.4, 30.1, 28.4
tBu[10]	89.6, 64.3, 63.8, 63.5, 63.5, 63.0, 62.6, 62.1, 61.6, 61.4, 30.1, 28.4

[a]Chemical shifts have been assigned previously by Bohlmann and Brehm on the basis of ^{13}C labeling experiments. See Fig. 5 for numbering scheme and ref. [37] for details.

UV/vis spectroscopy

A semi-empirical evaluation of the electronic landscape of polyynes can be obtained by UV/vis spectroscopic characterization. The UV/vis spectra of the **TIPS[*n*]** and **tBu[*n*]** polyynes are presented in Fig. 2, and λ_{max} values are summarized in Table 2. Several general points are worthy of comment:

1. The high-energy region of the UV/vis spectra (220–270 nm) of the longest polyynes ($n = 8$ and $n = 10$) is nearly transparent, a feature that stands out against most other conjugated organic oligomers.
2. The highest occupied molecular orbital–lowest unoccupied molecular orbital (HOMO–LUMO) transition dominates each spectrum, with vibronic structure unmistakably showing as a series of narrow absorption peaks with steadily increasing intensity toward the visible region.

3. The molar absorptivity (ε) steadily increases as the chain length increases, and ε values of **TIPS[10]** and **tBu[10]** are, for example, quite significant at ε = 753 000 and 736 000 L mol^{-1} cm^{-1}, respectively.
4. The choice of end-group has a noticeable effect on λ_{max} values for shorter polyynes, e.g., there is a range of 20 nm for tetraynes **TIPS[4]**, **Ad[4]**, and **tBu[4]** (λ_{max} = 260, 246, and 240 nm, respectively). The effect diminishes substantially for longer polyynes, e.g., there is only a range of 7 nm for decaynes **TIPS[10]**, **Ad[10]**, and **tBu[10]** (λ_{max} = 369, 367, and 362 nm, respectively).
5. There is a clear decrease in the HOMO → LUMO energy gap (E_g) vs. polyyne length.

Table 2 UV/vis spectroscopic data (λ_{max}) as measured in hexanes for the series **TIPS[*n*]**, **Ad[*n*]**, and **tBu[*n*]**.

n	**TIPS[*n*]** λ_{max} (nm)	**Ad[*n*]** λ_{max} (nm)	**tBu[*n*]** λ_{max} (nm)
3	234	–	213
4	260	246	240
5	284	272	266
6	306	295	289
8	339	335	330
10	369	367	362

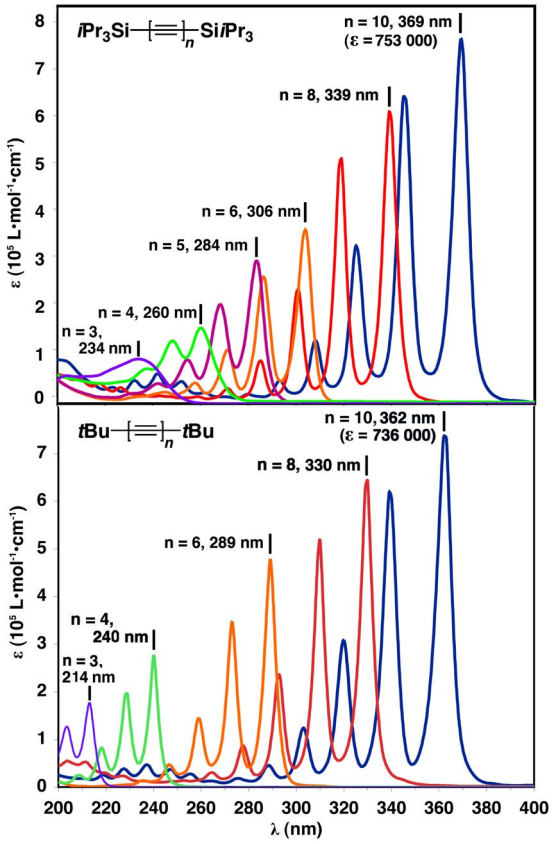

Fig. 2 UV/vis spectra for the series **TIPS[*n*]** and **tBu[*n*]** as measured in hexanes.

The final point above, (5), deserves elaboration. Considering electron correlation effects, the empirical power-law $E_g = 1/\lambda_{max} \sim n^{-x}$ can be used to describe the relationship between E_g, λ_{max} and n (where E_g is the energy of the HOMO → LUMO transition) [38–40]. This relationship is shown for **TIPS[*n*]**, **Ad[*n*]**, and **tBu[*n*]** in Fig. 3 for n = 3–10. In each case, there is a consistent power-law decrease in E_g through n = 10 that can be fit quite nicely for each series of polyynes **TIPS[*n*]** ($E_g \sim n^{-0.380}$), **Ad[*n*]** ($E_g \sim n^{-0.438}$), **tBu[*n*]** ($E_g \sim n^{-0.445}$) [41]. Despite small differences in the power-law relationship that presumably result from the varied end-capping groups, all values are close to the well-established "Lewis–Calvin Law" of $E_g \sim n^{-0.5}$ that has been documented for many conjugated materials [42,43]. It is worth emphasizing that for each case shown in Fig. 3, the power-law decrease in E_g includes all of the oligomers. Thus, for the trend of reduced HOMO → LUMO gap vs. length, saturation has not yet been reached.

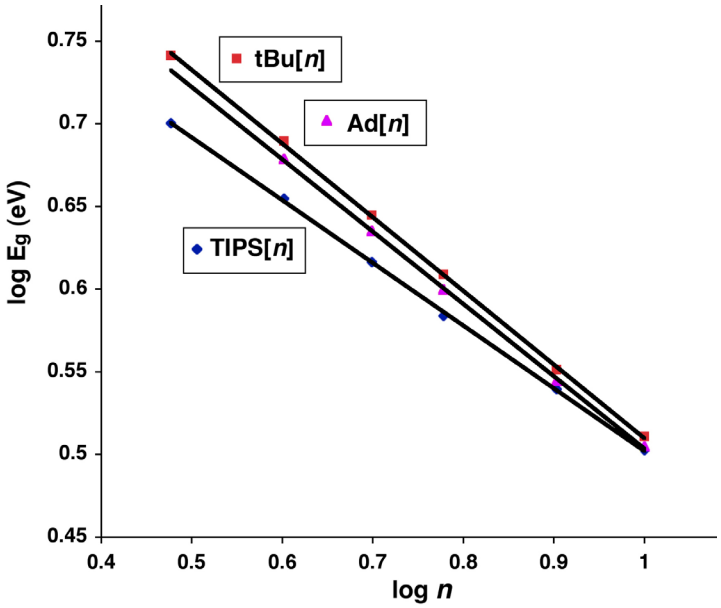

Fig. 3 Plot of log(E_g) vs. log(n) for **tBu[*n*]**, **Ad[*n*]**, and **TIPS[*n*]**. The solid line in each case represents the line-of-best-fit to the data (E_g is λ_{max} in eV).

Raman spectroscopy

Raman spectroscopy of polyynes **Ad[2]–Ad[10]** has been examined in THF solution and in the solid state [25]. As can be seen in Fig. 4 for the solid-state analysis, the spectra are very clean, and they are dominated by strong lines observed in the range of 1950–2300 cm^{-1}. These signals are conjugation-length dependent and can be assigned to the Я-mode [44–46] in the frame of the effective conjugation coordinate (ECC) theory of poly-conjugated chains [47,48]. In addition to the Я-mode, other lines observed above 600 cm^{-1} in the spectra are associated with the end-capping adamantyl groups [49]. Finally, several minor lines are found below 600 cm^{-1} and can be assigned to transversal and/or longitudinal vibrational modes of the polyyne chains [50,51].

The most obvious trend relayed from these analyses is that all Raman lines except the Я-mode rapidly disappear from the spectra as chain length increases and are nearly invisible by the stage of the tetrayne **Ad[4]**. This is due to the rapidly increasing Raman intensity of the Я-mode lines with chain length, which in the longer derivatives dominate the spectra. This dramatic increase of Raman intensity with chain length parallels what has been observed in polyenes [52]. Moreover, the Я-mode lines

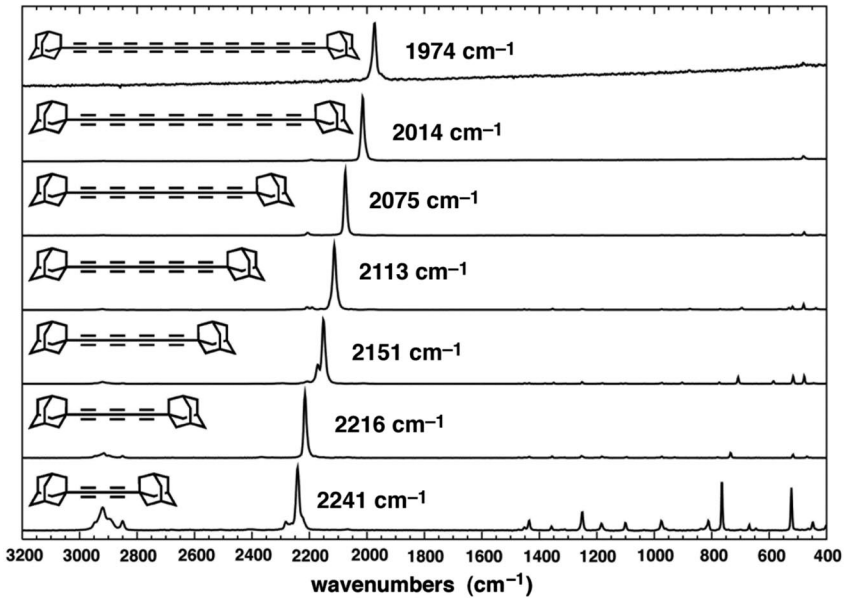

Fig. 4 Raman spectra as measured in the solid state for the series **Ad[*n*]**.

clearly show a red-shift in the Raman frequency as the number of C≡C bonds increases from **Ad[2]** (2241 cm^{-1}) to **Ad[10]** (1974 cm^{-1}), as predicted by the ECC model [45]. Thus, with increasing polyyne chain length, conjugation produces two noteworthy effects: (1) an increase of long-range interactions (which are at the basis of the *Я*-mode softening [46,53]), and (2) a decrease of BLA (i.e., an increase of the cumulenic character, toward the limit dictated by Peierls distortion [54], see also below) [55–57].

X-ray crystallography

While an indication of cumulenic character (reduced BLA) for longer polyynes is clear in the Raman spectra for the **Ad[*n*]** series, one of the most interesting questions in polyyne chemistry remains: Is there evidence of reduced BLA in the solid state? The answer to this question requires a set of X-ray crystallographic data that include polyynes with significant length, i.e., beyond that of a hexayne. Despite rather significant efforts (certainly within our group and likely within others), crystal structures of octaynes are rare, and there are no reports of X-ray data beyond the length of an octayne [16,24,58].

Despite the limited stability of the decayne **tBu[10]**, single crystals suitable for X-ray diffraction have been obtained by slow evaporation at 4 °C of a CH_2Cl_2 solution. The solid-state structure contains two crystallographically independent molecules in the unit cell, and these are labeled as molecule **tBu[10A]** and **tBu[10B]**, Figs. 5 and 6. Molecule **tBu[10A]** is not centrosymmetric and shows a helical conformation, while centrosymmetric molecule **tBu[10B]** adopts a gentle S-shape. Molecule **tBu[10A]** is the more strained of the two, with C–C≡C bond angles that range from 174.4(6)º to 179.3(5)º. Molecule **tBu[10B]** has a slightly smaller deviation from linearity, with C–C≡C bond angles that range from 176.1(6)º to 179.5(8)º. One of the most interesting features of the structure of decayne **tBu[10]** is its length: the molecule spans a remarkable 2.7 nm from end-to-end (i.e., C2A to C23A).

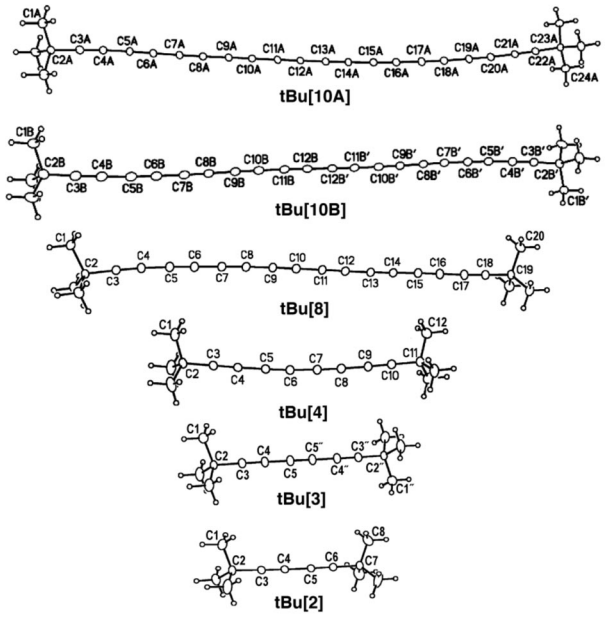

Fig. 5 ORTEP drawings (20 % probability level) for polyynes **tBu[2]**–**tBu[4]**, **tBu[8]**, **tBu[10A]**, and **tBu[10B]**.

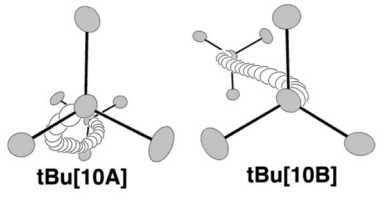

Fig. 6 End-on view of **tBu[10A]** and **tBu[10B]** highlighting the unique geometry of each molecule in the solid state (hydrogen atoms have been removed for clarity).

In addition to the structure of **tBu[10]**, crystal structures could also be obtained for diyne **tBu[2]**, triyne **tBu[3]**, tetrayne **tBu[4]**, and octayne **tBu[8]** [59]. With this extensive set of structural data available, there is an unprecedented opportunity to explore the prospect of reduced BLA as a function of increasing length [54,60,61]. The analysis of bond-length data from the crystallographic analysis of **tBu[*n*]** has been approached in two ways. First, as is common for computed structures (e.g., Table 3, entries 13–17), BLA has been calculated as the bond-length difference between the central single and triple bonds in each structure. In cases where the polyyne structure is non-centrosymmetric in the solid state, positionally equivalent bonds have been averaged {i.e., BLA (**tBu[2]**) = (C4–C5) – [(C3≡C4) + (C5≡C6)]/2}. This analysis of BLA shows a consistent reduction in values from a maximum of 0.184 Å (dimer **tBu[2]**) to a minimum of 0.139 Å (average of **tBu[10A]** and **tBu[10B]**). BLA analysis over the range of molecules examined here suggests that the reduction in BLA is approaching saturation somewhere in the range of BLA = 0.135 Å (Fig. 7). A potential issue with this basic analysis of bond-length changes as a function of length is, however, that it focuses on the difference of two specific bonds. Thus, it is possible that small experimental errors in either of these bond-length values might distort comparisons with other BLA values. In an attempt to minimize such an error, the difference between the average of all single and triple bonds, BLA_{avg}, has also been examined [26]. Similar to the pure BLA values, BLA_{avg} values decrease steadily as a function of length for **tBu[*n*]**, and the onset of saturation is also evident at the stage of the decayne (Fig. 7).

Table 3 Details of experimental and theoretical BLA data.

Entry	Polyyne	BLA[a] (Å)	BLA_{avg}[b] (Å)	References
1	**tBu[2]**	0.184	0.183	[26]
2	**tBu[3]**	0.164	0.166	[26]
3	**tBu[4]**	0.151	0.161	[5,26]
4	**tBu[8]**	0.140	0.147	[26]
5	**tBu[10A]**	0.144	0.143	[26]
6	**tBu[10B]**	0.134	0.148	[26]
7	**$tBu[10]_{avg}$**	0.139	0.146	[26]
8	**TIPS[2]**	0.169	0.169	[68]
9	**TIPS[4]**	0.157	0.157	[24]
10	**TIPS[5]**	0.148	0.153	[24]
11	**TIPS[6]**	0.149	0.153	[24]
12	**TIPS[8]**	0.153	0.161	[24]
13	$H\text{-}(C{\equiv}C)_9\text{-}H$	0.1291[c]	0.13675	[62]
14	$H\text{-}(C{\equiv}C)_\infty\text{-}H$	0.1276[c]	–	[62]
15	$H\text{-}(C{\equiv}C)_\infty\text{-}H$	0.133[d]	–	[65]
16	$H\text{-}(C{\equiv}C)_\infty\text{-}H$	0.131[e]	–	[65]
17	$H\text{-}(C{\equiv}C)_\infty\text{-}H$	0.134[f]	–	[64]

[a]See text.
[b]$[C\text{–}C_{avg}] - [C{\equiv}C_{avg}]$; note: calculation does not include terminal C–C bond (e.g., C2–C3).
[c]Calculated at CCSD(T)/cc-PVTZ level of theory.
[d]Results from BHHLYP functional.
[e]Results from CAM-B3LYP functional.
[f]Results from B3LYP//BH&HLYP functional.

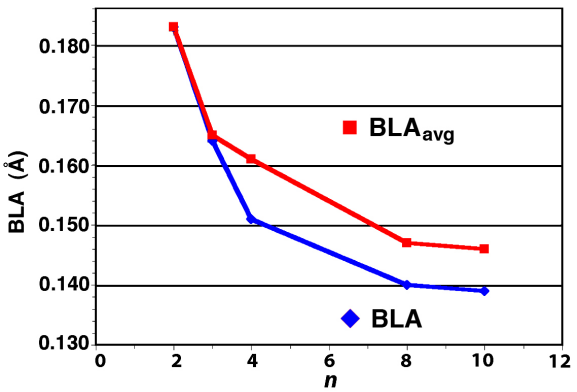

Fig. 7 Graph of BLA (◆) and BLA_{avg} (■) vs. *n* for the series **tBu[*n*]**.

With limited X-ray data available for longer polyynes without metal end-groups [58], comparison of BLA trends observed for the series **tBu[*n*]** to other systems is difficult. The silyl end-capped polyynes **TIPS[*n*]** offer one possibility, as shown in entries 8–12 of Table 2. For the **TIPS[*n*]** molecules, there is clearly an overall reduction in both BLA values as one moves from diyne **TIPS[2]** (0.169 Å) to octayne **TIPS[8]** (0.153 Å). On closer inspection, however, it is noted that neither the individual values nor the overall trend compare well with the data for **tBu[*n*]**. Remarkable is the fact that BLA_{avg} data for molecules **TIPS[*n*]** shows no real trend at all, and it is quite likely that this originates from an end-

group effect. Given the electronic interaction of the polyynes with the triisopropylsilyl moiety, there appears to be a slight reduction in the BLA toward the termini of the polyyne. In the shorter **TIPS[*n*]** derivatives, this affords a smaller apparent BLA_{avg} value and negates the establishment of a trend.

As described above, the experimental study of BLA for polyynes has been limited to date. Computational chemists have, on the other hand, frequently addressed this question for polyynes, and these recent theoretical studies have noted that the choice of basis set and electron correlation have a dramatic effect on results [62–67]. These reports do, however, predict that BLA values should converge to a value of ca. 0.13 Å (Table 3, entries 13–17) [62,64,65], which is a value remarkably close to that estimated from the data for **tBu[*n*]**. Furthermore, a comparison of BLA and BLA_{avg} for **tBu[8]** and **tBu[10]** with those predicted theoretically for H-$(C{\equiv}C)_9$-H (entry 13) shows a difference of only ca. 0.01 Å. Thus, there is overall very good agreement between the experimental values and those predicted by various levels of theory. As a final point, it should be noted that there is sufficient error in each experimental BLA value to make individual comparisons risky in some cases. The overall trend in experimental data, however, clearly points to a reduced BLA as a function of length [26].

CONCLUSIONS: WHERE TO NOW?

The studies outlined above offer some insight into the properties of polyyne oligomers as well as the possible properties of carbyne. BLA studies for the series **tBu[*n*]** may even indicate that saturation of properties is on the horizon. There is, however, one overwhelming conclusion from the synthesis and study of the three series of polyynes **tBu[*n*]**, **Ad[*n*]**, and **TIPS[*n*]**: In each case, molecules beyond the length of a decayne have been untenable. Conventional wisdom suggests that this is a result of the similar size of the three end-capping groups, which limits the extent of steric hindrance that might prevent intermolecular interactions that degenerate into decomposition. As can be seen in Fig. 8, there is indeed

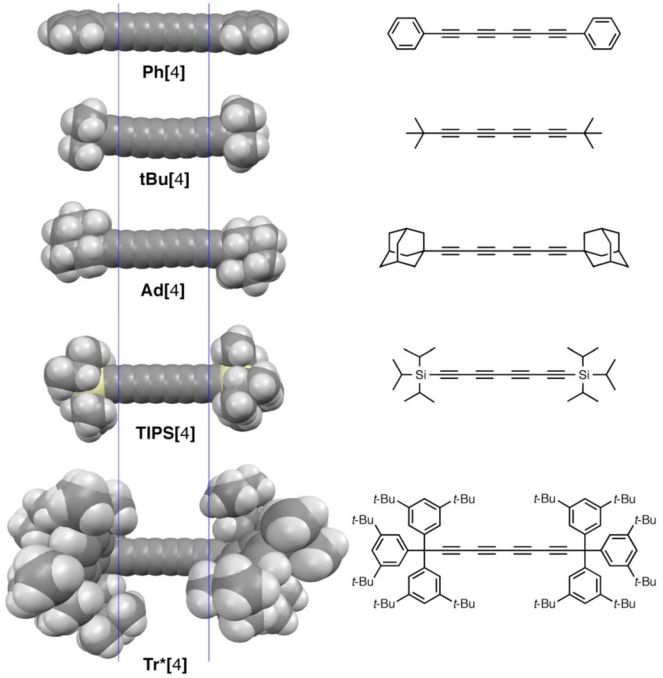

Fig. 8 Schematic comparison of steric bulk of several tetraynes, including (from top to bottom) **Ph[4]**, **tBu[4]**, **Ad[4]**, **TIPS[4]**, **Tr*[4]** based on X-ray crystallographic data [72]. The two lines are simply a guide to the eye, drawn at the C(1)–C(2) and C(7)–C(8) bond in each case.

little difference in size between **tBu[4]** [26], **Ad[4]** [25], and **TIPS[4]** [24]. This premise is also supported by the fact that analysis of the **Ph[*n*]** series of molecules, which feature an even smaller end-capping group (e.g., see **Ph[4]** [69] Fig. 1), was limited only to the octayne **Ph[8]** [10,70]. Thus, a larger end-capping group is needed. After experimenting with several options, current efforts have been directed toward the incorporation of a "super trityl" group. This end-capping group features a diameter that is more than double that of *t*-Bu, Ad, or TIPS groups, as can be appreciated from looking at **Tr*[4]** [71] (Fig. 8). Particularly impressive is the shielding of the carbon chain by the Tr* groups, which extends over at least the 2–3 end-most acetylenic carbons. The results of this investigation are promising and will be reported in due course.

ACKNOWLEDGMENTS

We are grateful for the generous financial support as provided by the University of Alberta and the Natural Sciences and Engineering Research Council of Canada (NSERC). We thank Drs. Bob McDonald and Michael J. Ferguson for solving the numerous crystal structures that contributed greatly to this work and Dr. Eike Jahnke for helpful discussions.

REFERENCES AND NOTES

1. E. H. L. Falcao, F. Wudl. *J. Chem. Technol. Biotechnol.* **82**, 524 (2007).
2. R. B. Heimann, S. E. Evsyukov, L. Kavan (Eds.). *Carbyne and Carbynoid Structures*, Springer, Berlin (1999).
3. F. Cataldo (Ed.). *Polyynes: Synthesis, Properies, and Applications*, Taylor & Francis, Boca Raton (2006).
4. P. P. K. Smith, P. R. Buseck. *Science* **216**, 984 (1982).
5. R. J. Lagow, J. J. Kampa, H.-C. Wei, S. L. Battle, J. W. Gegne, D. A. Laude, C. J. Harper, R. Bau, R. C. Stevens, J. F. Haw, E. Munson. *Science* **267**, 362 (1995).
6. K. Müllen, G. Wegner (Eds.). *Electronic Materials: The Oligomer Approach*, Wiley-VCH, Weinheim (1998).
7. R. E. Martin, F. Diederich. *Angew. Chem., Int. Ed.* **38**, 1350 (1999).
8. F. Bohlmann. *Chem. Ber.* **86**, 657 (1953).
9. E. R. H. Jones, H. H. Lee, M. C. Whiting. *J. Chem. Soc.* 3483 (1960).
10. T. R. Johnson, D. R. M. Walton. *Tetrahedron* **28**, 5221 (1972).
11. R. Eastmond, T. R. Johnson, D. R. M. Walton. *Tetrahedron* **28**, 4601 (1972).
12. S. M. E. Simpkins, M. D. Weller, L. R. Cox. *Chem. Commun.* 4035 (2007).
13. W. A. Chalifoux, R. R. Tykwinski. *C.R. Chim.* **12**, 341 (2009).
14. Y. Tobe, T. Wakabayashi. In *Acetylene Chemistry: Chemistry, Biology, and Material Science*, F. Diederich, P. J. Stang, R. R. Tykwinski (Eds.), Chap. 9, Wiley-VCH, Weinheim, Germany (2005).
15. W. A. Chalifoux, R. R. Tykwinski. *Chem. Rec.* **6**, 169 (2006).
16. W. Mohr, J. Stahl, F. Hampel, J. A. Gladysz. *Chem.—Eur. J.* **9**, 3324 (2003).
17. Q. Zheng, J. A. Gladysz. *J. Am. Chem. Soc.* **127**, 10508 (2005).
18. Q. Zheng, J. C. Bohling, T. B. Peters, A. C. Frisch, F. Hampel, J. A. Gladysz. *Chem.—Eur. J.* **12**, 6486 (2006).
19. M. Samoc, G. T. Dalton, J. A. Gladysz, Q. Zheng, Y. Velkov, H. Ågren, P. Norman, M. G. Humphrey. *Inorg. Chem.* **47**, 9946 (2008).
20. (a) P. Fritsch. *Liebigs Ann. Chem.* **279**, 319 (1894); (b) W. P. Buttenberg. *Liebigs Ann. Chem.* **279**, 324 (1894); (c) H. Wiechell. *Liebigs Ann. Chem.* **279**, 337 (1894).
21. For reviews, see: (a) R. Knorr. *Chem. Rev.* **104**, 3795 (2004); (b) W. Kirmse. *Angew. Chem., Int. Ed.* **36**, 1164 (1997); (c) P. J. Stang. *Chem. Rev.* **78**, 383 (1978).

22. For recent examples of polyyne syntheses using the FBW rearrangement, see: (a) P. Bichler, W. A. Chalifoux, S. Eisler, A. L. K. Shi Shun, E. T. Chernick, R. R. Tykwinski. *Org. Lett.* **11**, 519 (2009); (b) M. Ochiai. *Synlett* 159 (2009); (c) A. Spantulescu, T. Luu, Y. Zhao, R. McDonald, R. R. Tykwinski. *Org. Lett.* **10**, 609 (2008); (d) J. Kendall, R. McDonald, M. J. Ferguson, R. R. Tykwinski. *Org. Lett.* **10**, 2163 (2008); (e) T. Luu, Y. Morisaki, N. Cunningham, R. R. Tykwinski. *J. Org. Chem.* **72**, 9622 (2007); (f) Y. Tobe, R. Umeda, N. Iwasa, M. Sonoda. *Chem.—Eur. J.* **9**, 5549 (2003).
23. A. D. Slepkov, F. A. Hegmann, S. Eisler, E. Elliott, R. R. Tykwinski. *J. Chem. Phys.* **120**, 6807 (2004).
24. S. Eisler, A. D. Slepkov, E. Elliott, T. Luu, R. McDonald, F. A. Hegmann, R. R. Tykwinski. *J. Am. Chem. Soc.* **127**, 2666 (2005).
25. A. Lucotti, M. Tommasini, D. Fazzi, M. Del Zoppo, W. A. Chalifoux, M. J. Ferguson, G. Zerbi, R. R. Tykwinski. *J. Am. Chem. Soc.* **131**, 4239 (2009).
26. W. A. Chalifoux, R. McDonald, M. J. Ferguson, R. R. Tykwinski. *Angew. Chem., Int. Ed.* **48**, 7915 (2009).
27. S. Eisler, R. R. Tykwinski. *J. Am. Chem. Soc.* **122**, 10736 (2000).
28. J.-H. Li, Y. Liang, Y.-X. Xie. *J. Org. Chem.* **70**, 4393 (2005).
29. A. L. K. Shi Shun, E. T. Chernick, S. Eisler, R. R. Tykwinski. *J. Org. Chem.* **68**, 1339 (2003).
30. S. Eisler, N. Chahal, R. McDonald, R. R. Tykwinski. *Chem.—Eur. J.* **9**, 2542 (2003).
31. (a) F. Ramirez, N. B. Desai, N. McKelvie. *J. Am. Chem. Soc.* **84**, 1745 (1962); (b) E. J. Corey, P. L. Fuchs. *Tetrahedron Lett.* **13**, 3769 (1972).
32. (a) C. Moureu, R. Delange. *Bull. Soc. Chim. Fr*. 648 (1903); (b) G. H. Mansfield, M. C. Whiting. *J. Chem. Soc.* 4761 (1956); (c) R. Knorr, C. Pires, C. Behringer, T. Menke, J. Freudenreich, E. C. Rossmann, P. Böhrer. *J. Am. Chem. Soc*. **128**, 14845 (2006).
33. D. R. M. Walton, F. Waugh. *J. Organomet. Chem.* **37**, 45 (1972).
34. A. S. Hay. *J. Org. Chem.* **27**, 3320 (1962).
35. T. Gibtner, F. Hampel, J.-P. Gisselbrecht, A. Hirsch. *Chem.—Eur. J.* **8**, 408 (2002).
36. G. Eglinton, A. R. Galbraith. *Chem. Ind. (London)* 7378 (1956).
37. F. Bohlmann, M. Brehm. *Chem. Ber.* **112**, 1071 (1979).
38. C. Bubeck. In *Electronic Materials: The Oligomer Approach*, K. Müllen, G. Wegner (Eds.), Chap. 8, Wiley-VCH, Weinheim (1998).
39. Y. Luo, P. Norman, K. Ruud, H. Ågren. *Chem. Phys. Lett.* **285**, 160 (1998).
40. A. Mathy, K. Ueberhofen, R. Schenk, H. Gregorius, R. Garay, K. Müllen, C. Bubeck. *Phys. Rev. B* **53**, 4367 (1996).
41. In each case, $R^2 \geq 0.9996$.
42. G. N. Lewis, M. Calvin. *Chem. Rev.* **25**, 273 (1939).
43. For examples of analysis of polyyne HOMO-LUMO gaps using the Lewis–Calvin approach, see: (a) refs. [10,11,24]; (b) J. B. Armitage, N. Entwistle, E. R. H. Jones, M. C. Whiting. *J. Chem. Soc.* 147 (1954); (c) G. Schermann, T. Grösser, F. Hampel, A. Hirsch. *Chem.—Eur. J.* **3**, 1105 (1997).
44. A. Milani, M. Tommasini, M. Del Zoppo, C. Castiglioni, G. Zerbi. *Phys. Rev. B* **74**, 153418 (2006).
45. M. Tommasini, D. Fazzi, A. Milani, M. Del Zoppo, C. Castiglioni, G. Zerbi. *J. Phys. Chem. A* **111**, 11645 (2007).
46. M. Tommasini, A. Milani, D. Fazzi, M. Del Zoppo, C. Castiglioni, G. Zerbi. *Physica E* **40**, 2570 (2008).
47. C. Castiglioni, M. Tommasini, G. Zerbi. *Philos. Trans. R. Soc. Lond. A* **362**, 2425 (2004).
48. C. Castiglioni, J. T. L. Navarrete, G. Zerbi, M. Gussoni. *Solid State Commun.* **65**, 625 (1988).
49. J. O. Jensen. *Spectrochim. Acta, Part A* **60**, 1895 (2004).
50. C. S. Casari, A. Li Bassi, A. Baserga, L. Ravagnan, P. Piseri, C. Lenardi, M. Tommasini, A. Milani, D. Fazzi, C. E. Bottani, P. Milani. *Phys. Rev. B* **77**, 195444 (2008).

51. J. Neugebauer, M. Reiher. *J. Phys. Chem. A* **108**, 2053 (2004).
52. M. Del Zoppo, C. Castiglioni, P. Zuliani, G. Zerbi. *Synth. Met*. **85**, 1043 (1997).
53. A. Milani, M. Tommasini, G. Zerbi. *J. Chem. Phys.* **128**, 064501 (2008).
54. A. Milani, M. Tommasini, D. Fazzi, C. Castiglioni, M. Del Zoppo, G. Zerbi. *J. Raman Spectrosc.* **39**, 164 (2008).
55. Increased cumulenic character vs. polyyne length based on Raman spectroscopy has been noted previously. For the study of polyynes by Raman spectroscopy, see refs. [56,57].
56. Raman spectroscopy: (a) ref. [35]; (b) H. Tabata, M. Fujii, S. Hayashi, T. Doi, T. Wakabayashi. *Carbon* **44**, 3168 (2006); (c) R. Dembinski, T. Bartik, B. Bartik, M. Jaeger, J. A. Gladysz. *J. Am. Chem. Soc.* **122**, 810 (2000).
57. SERS: (a) ref. [56b]; (b) C. S. Casari, V. Russo, A. Li Bassi, C. E. Bottani, F. Cataldo, A. Lucotti, M. Tommasini, M. Del Zoppo, C. Castiglioni, G. Zerbi. *Appl. Phys. Lett.* **90**, 013111 (2007); (c) A. Lucotti, M. Tommasini, M. Del Zoppo, C. Castiglioni, G. Zerbi, F. Cataldo, C. S. Casari, A. Li Bassi, V. Russo, M. Bogana, C. E. Bottani. *Chem. Phys. Lett.* **417**, 78 (2006).
58. S. Szafert, J. A. Gladysz. *Chem. Rev.* **106**, PR1 (2006).
59. CCDC Nos: 729156 (**tBu[2]**), 729157 (**tBu[3]**), 729158 (**tBu[4]**), 729159 (**tBu[8]**), 729160 (**tBu[10]**).
60. M. Kertesz, C. H. Choi, S. Yang. *Chem. Rev.* **105**, 3448 (2005).
61. R. Hoffmann. *Angew. Chem., Int. Ed. Engl.* **26**, 846 (1987).
62. C. D. Zeinalipour-Yazdi, D. P. Pullman. *J. Phys. Chem. B* **112**, 7377 (2008).
63. S. Yang, M. Kertesz, V. Zólyomi, J. Kürti. *J. Phys. Chem. A* **111**, 2434 (2007).
64. S. Yang, M. Kertesz. *J. Phys. Chem. A* **110**, 9771 (2006).
65. M. J. G. Peach, E. I. Tellgren, P. Salek, T. Helgaker, D. J. Tozer. *J. Phys. Chem. A* **111**, 11930 (2007).
66. A. Scemama, P. Chaquin, M.-C. Gazeau, Y. Bénilan. *J. Phys. Chem. A* **106**, 3828 (2002).
67. L. Horny, N. D. K. Petraco, C. Pak, H. F. Schaefer III. *J. Am. Chem. Soc.* **124**, 5861 (2002).
68. E. C. Constable, D. Gusmeroli, C. E. Housecroft, M. Neuburger, S. Schaffner. *Acta Crystallogr., Sect. C: Cryst. Struct. Commun.* **62**, O505 (2006).
69. Crystallographic data for **Ph[4]** ($C_{20}H_{10}$), M_W = 250.28; monoclinic crystal system; space group $P2_1/n$ (an alternate setting of $P2_1/c$ [No. 14]), a = 10.7824(12), b = 3.9194(5), c = 16.901(2) Å; σ = 106.0485(17)°; V = 686.39(14) Å^3; Z = 2; ρ_{calcd} = 1.211 g cm^{-3}; μ = 0.069 mm^{-1}; λ = 0.71073 Å; T = –80 °C; 2θmax = 52.80°; total data collected = 4905; R_1 = 0.0361 for 1179 observed reflections with [$F_o^2 \geq 2\sigma(F_o^2)$]; wR_2 = 0.1041 for 92 variables and 1404 unique reflections with [$F_o^2 \geq -3\sigma(F_o^2)$]; residual electron density = 0.130 and –0.140 e Å^{-3}.
70. T. Luu, E. Elliott, A. D. Slepkov, S. Eisler, R. McDonald, F. A. Hegmann, R. R. Tykwinski. *Org. Lett.* **7**, 51 (2005).
71. Crystallographic data for **Tr*[4]** ($C_{94}H_{126}$·0.5$C_4H_{10}O$), M_W = 1293.01; monoclinic crystal system; space group $P2_1/n$ (an alternate setting of $P2_1/c$ [No. 14]); a = 28.705(9), b = 10.621(3), c = 29.280(9) Å; β = 92.763(4)°; V = 8916(5) Å^3; Z = 4; ρ_{calcd} = 0.963 g cm^{-3}; μ = 0.054 mm^{-1}; λ = 0.71073 Å; T = –100 °C; 2θmax = 50.50°; total data collected = 61984; R_1 = 0.0584 for 16159 observed reflections with [$F_o^2 \geq -2\sigma(F_o^2)$]; wR_2 = 0.1699 for 962 variables and 16159 unique reflections with [$F_o^2 \geq -3\sigma(F_o^2)$], and 14 restraints [The disordered diethylether solvent molecules had the following distance restraints applied: O–C restrained to be 1.430(2) Å; C–C, 1.530(2) Å; C···C, 2.340(4) Å; O···C, 2.420(4) Å]; residual electron density = 0.376 and –0.297 e Å^{-3}.
72. CCDC Nos: 745804 (**Ph[4]**), 729158 (**tBu**[**4**]), 660940 (**Ad[4]**), 265860 (**TIPS[4]**), and 745805 (**Tr*[4]**).

